Characterization and Properties of the Neutral and Doped Blends of Poly(3-dodecylthiophene) with Low-Density Polyethylene

XIUYING QIAO, XIANHONG WANG, XIAOJIANG ZHAO, YANJU WANG, QINGYONG CHEN, ZHISHEN MO

State Key Laboratory of Polymer Physics and Chemistry, Changchun Institute of Applied Chemistry, Chinese Academy of Sciences, Changchun 130022, P. R.China

Received 19 March 2001; accepted 5 July 2001

ABSTRACT: In this paper, the structures and properties of the neutral and doped blends of poly(3-dodecylthiophene) (P3DDT) with low-density polyethylene (LDPE) were investigated. Wide-angle X-ray diffraction (WAXD), differential scanning calorimetry (DSC), Fourier transform infrared spectra (FTIR), and scanning electron microscopy (SEM) were used to characterize the structures and morphologies of the blends, and conductivity was also measured. It was found that separate crystallizations occur between P3DDT and LDPE. When the amount of P3DDT is small in the blend, it has the effect of a nucleation reagent and has some influence on the crystal structure. After doping, the interaction force between the molecular chains increases, and leads to a more compact packing and a more uniform dispersion in morphology. Through blending, the thermal stability of pure component could be greatly improved, especially when the P3DDT content is 5 wt %. The conductivity measurements indicate that the conductivity increases with the increase of the P3DDT composition and doping time.
 J Appl Polym Sci 84: 741–749, 2002; DOI 10.1002/app.10247

Key words: conductivity; structure; blends; poly(3-dodecylthiophene); low-density polyethylene

INTRODUCTION

Polymers containing highly loosely held electrons in their backbones are often referred to as conjugated polymers or conducting polymers. The investigation for conducting polymers began with polyacetylene at the end of 1970s,[1] then followed by polypyrrole,[2] polyaniline,[3,4] polythiophene,[5–7] and so on. It is the existence of delocalization of electrons along the polymer backbone that makes these systems behave as an electrical conductor. However, due to the intractability and insolubility, the application of conducting polymers has been limited for some time. In this case, poly(3-alkylthiophenes) (P3ATs), as a kind of highly soluble, fusible and processable conducting polymers, [8–11] have attracted great attention and motivated intense research and development. It has been widely accepted that P3ATs can form similar layered structures with side chains acting as spacers.

In order to extend the commercial utilization of these promising conductive polymers, many researchers have developed the investigation of the blends of P3ATs and other conventional melt-processable polymers.[12–14] By blending, that is to

Correspondence to: Z. Mo (mozs@ciac.jl.cn).
Contract grant sponsors: Special Funds for Major State Basic Research Projects; Chinese "863-2" High Technology Funds.

Journal of Applied Polymer Science, Vol. 84, 741–749 (2002)

say, the decrease in the amount of the conducting polymer, the improvement of the mechanical properties and the lowering of the price could then be obtained. In this study, poly(3-dodecylthiophene) (P3DDT) was used to blend with low-density polyethylene (LDPE), and the properties of the resultant blends were also investigated under their both neutral and doped states.

EXPERIMENTAL

Materials and Preparation

P3DDT was synthesized chemically via the polymerization of the monomers.[6] The preparation of the monomers takes advantage of the Ni(DPPP)Cl_2 catalyzed cross-coupling reaction between 3-bromothiophene and Grignard reagents derived from alkyl bromide,[15] while the polymerization was done in chloroform solution at room temperature under a nitrogen purge. The polymer, obtained from the precipitation of the reactant in methanol, was first washed with methanol until the solution appeared colorless, and then was dried in vacuum at 40°C. The weight-average molecular weight ($\overline{M}_w$) and number-average molecular weight ($\overline{M}_n$) of P3DDT were obtained as $\overline{M}_w = 6.9 \times 10^4$ and $\overline{M}_n = 2.0 \times 10^4$ with a polydispersity index of 3.5 by gel permeation chromatography (GPC). Low-density polyethylene in this study is an industrialization product from Beijing Yanshan petrochemical plant (1I2A-1).

Blends of P3DDT and LDPE, with the wt % ratios of 0.5, 1, 5, 10, and 20 of P3DDT, were made by melt extrusion at 160°C. These blends were then defined as 0.5/99.5, 1/99, 5/95, 10/90, and 20/80 blends, just as called in this paper. Films of LDPE and the blends were made by the use of compression molding at 160°C at 50 bar for 3min and then cooled at room temperature. Film of P3DDT was made by the evaporation of the 2 wt % solution of $CHCl_3$ at room temperature. And then the films of the blends and P3DDT were doped by immersion in 0.1*M* nitromethane solutions of anhydrous ferric chloride, and then washed with dry nitromethane and dried in vacuum for measurements.

Measurements

Wide-angle X-ray diffraction (WAXD) experiments were carried out by the use of Rigaku D/Max-II B X-ray diffractometer with a Cu anode ($CuK_{\alpha 1}$ = 1.5406 Å). The measurements were operated at 40 kV and 20 mA from 2°–40° at a 2θ scan rate of 4°C/min.

Perking-Elmer DSC-7 calibrated with indium standard was used for the measurements of differential scanning calorimetry (DSC). The measurements were performed at the atmosphere of nitrogen. The samples, typically 6 mg, were heated from 0 to 180°C at 10°C/min. A Perkin-Elmer thermal gravity analysis (TGA) was also used to investigate the thermal stability of these samples in the air. The measurements were carried out in a temperature range from 20 to 800°C with a scanning rate of 10°C/min.

Bio-Rad FTS-60 Fourier transform infrared spectrometer was used to record the Fourier infrared spectra ranging between the wavenumber of 400 and 4000 cm^{-1} at room temperature.

The morphology of the blends was studied with a Jeol JEX-840 Scanning Electron Microscope operated at 20 kV. The cryofractured samples from melt extrusion were coated with a thin gold layer prior to measurements.

Conductivity measurements were done for the doped samples by the use of a four probe method.

All the measurements mentioned above were done at ambient temperature in laboratory atmosphere.

RESULTS AND DISCUSSION

Wide Angle X-ray Diffraction

The X-ray diffraction patterns of the neutral and doped P3DDT/LDPE blends are given in Figure 1. For the neutral P3DDT/LDPE blends, it can be observed in Figure 1(a) that there are obvious (110) and (200) reflections of LDPE at wide angle for all the blends. For the 0.5/99.5, 1/99, and 5/95 blends, a peak centered at around 25.7° becomes more evident. Its being more intensive can be attributed to the effect of minor P3DDT as a nucleation reagent. When the amount of P3DDT is no less than 5%, the (100) reflection of P3DDT at small angle becomes obvious and turns intensive with the increase of P3DDT content.

The characteristic reflection peaks of LDPE keep almost the same position when the composition varies, but the *d*-spacing value of (100) diffraction peak of P3DDT turns greater after blending. The X-ray diffraction patterns of the blends show the separate characteristic diffraction of the composition, thus suggesting the sep-

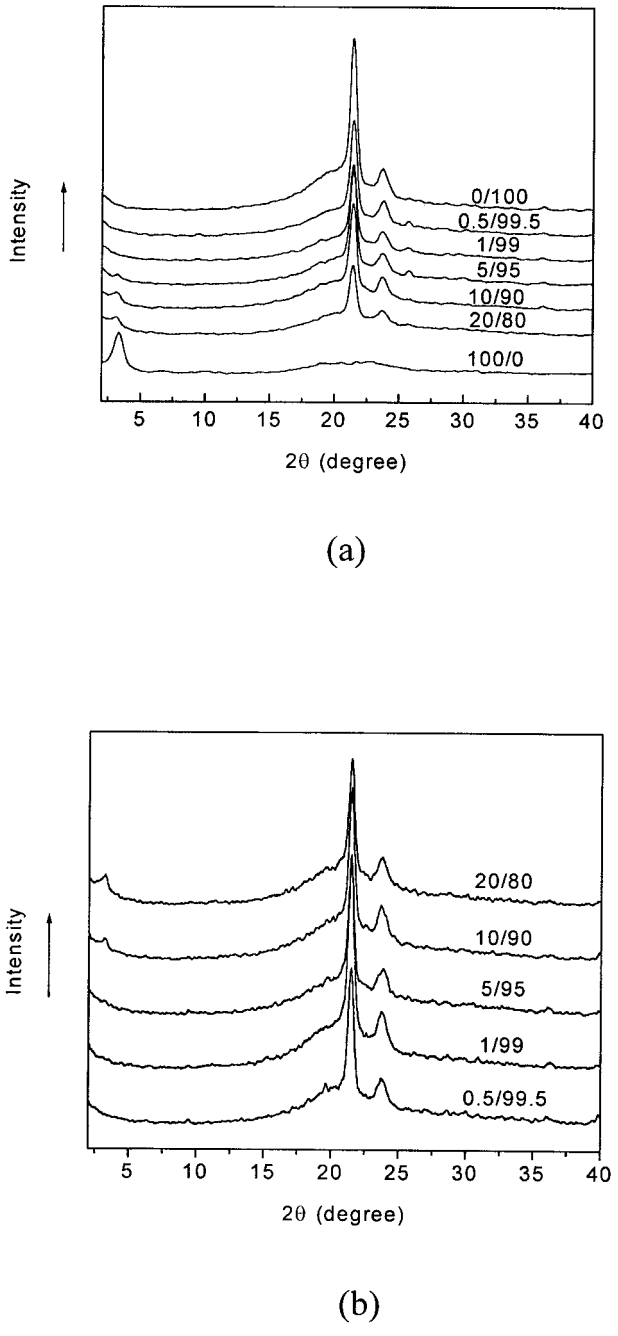

Figure 1 X-ray diffraction patterns of the neutral and doped P3DDT/LDPE blends: (a) the neutral blends; (b) the doped blends.

arate crystallization of the composition. During the rapid cooling process at room temperature, LDPE can crystallize before P3DDT can; the segments of LDPE having been rearranged regularly will have some limits to the packing of the molecular chains of P3DDT. The left shifts of the (100) planes of the blends, compared with the pure P3DDT, can be thought of as resulting from the limits of the crystallized segments of LDPE.

It is clear in Figure 1(b) that after doping, almost no change takes place as to the shape of the diffraction peaks except that the (100) reflection of P3DDT has some decrease in intensity and even negligible. In addition, after doping, the *d*-spacing values of the diffraction peaks of LDPE have almost no change, and the d spacing of (100) plane of P3DDT have some decrement. In the doping process, negative $FeCl^{4-}$ ions are formed as the counterions for the positively charged polymer chains.[16] Doping reaction takes place between the counterions and P3DDT, thus making the *d*-spacing value of (100) plane in P3DDT have the greatest changes. Once polarons and bipolarons are generated on the conjugation system upon the doping, the interaction between neighboring main chains will become stronger, thus resulting in the decrease in the *d*-spacing between the adjacent crystalline planes. It has been demonstrated that the dopant ions within the doped crystal structure lie to between the alkyl chain and the neighboring thiophene ring.[17] Meanwhile, it can be assumed that the weakness and even disappearance of the (100) reflection should be related to the structural repositioning of the molecular chains in P3DDT due to the intervention of dopant.

Thermal Analysis

Melting curves obtained by DSC for the neutral and doped P3DDT/LDPE blends are shown in Figure 2. As for the neutral P3DDT/LDPE blends, in the first heating run, there are one weak peak located at around 39°C and one strong peak at around 105°C for each blend and the pure LDPE. In addition, there is also a shoulder peak additional to the high-temperature peak for each blend, except the blend containing 20% of P3DDT. It can be observed that with the increase of the amount of P3DDT in the blend, the high temperature peak becomes sharper and shifts a little to higher temperature. Meanwhile, the shoulder peak becomes weaker and finally disappears for the 20/80 blend, but its position keeps almost the same as the composition varies. The low temperature peaks for the pure LDPE and the blend can be attributed to the thermal history due to rapid cooling process, which can be demonstrated by the disappearance of these peaks in the second heating scan. As for the shoulder peaks, it appears that they are probably due to the melting

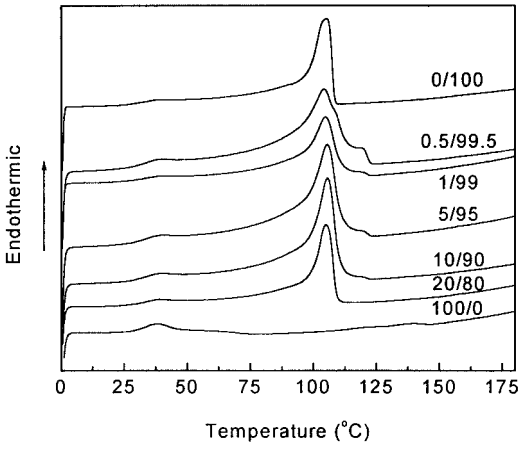

(a)

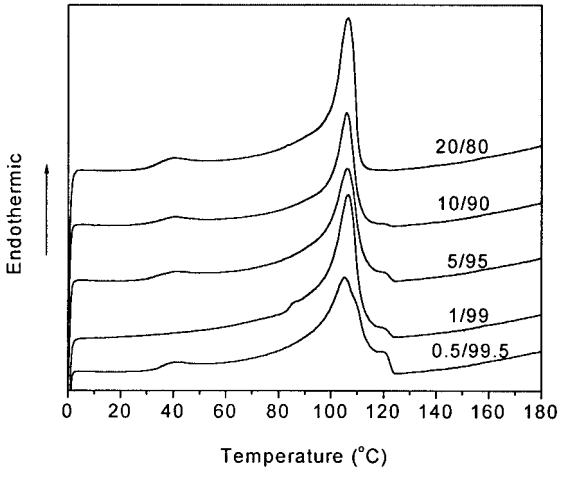

(b)

Figure 2 Melting DSC curves for the neutral and doped P3DDT/LDPE blends: (a) the neutral blends; (b) the doped blends.

endotherms of the recrystallized LDPE that are nucleated by the minor amount of P3DDT. However, during the melting of P3DDT/LDPE blends, there are no obvious melting endotherms of P3DDT, which can be easily understood out of the considerations of the weak melting endothermic peaks of P3DDT.

Compared with Figure 2(a), the shapes of the DSC curves in Figure 2(b) are almost the same as those in Figure 2(a). This phenomenon suggests that the doping process should have no great effect on the structures of the crystalline phases of the blends. Nevertheless, after doping, the melting and crystallization temperatures turn greater. The addition of the dopant can increase the polarity of molecular chains, then increase the interaction force between the molecular chains, and then increase the energy needed for melting and decrease the energy needed for crystallization.

In general, thermal gravity analysis plays a very important role in the investigation of the thermal stability of functional materials. The results of thermogravimetric analysis of the neutral P3DDT/LDPE blends are shown in Figure 3. It can be observed that the first onset decomposition temperatures are 235.5°C for LDPE, 246.9°C for 0.5/99.5 blend, 263.5°C for 1/99 blend, 287.8°C for 5/95 blend, 287.0°C for 10/90 blend, 245.4°C for 20/80 blend, and 263.0°C for P3DDT, respectively. While the second onset decomposition temperatures are 419.2°C for 0.5/99.5 blend, 421.7°C for 1/99 blend, 422.1°C for 5/95 blend, 407.0°C for 10/90 blend, and 392.6°C for 20/80 blend, respectively. During the first decomposition process, for the pure LDPE, the maximum decomposition is 50.23 wt % at 365.9°C; for the pure P3DDT, the maximum decomposition is 11.10 wt % at 309.9°C; for the 20/80 blend, the maximum decomposition is 11.46 wt % at 291.7°C. However, for the other P3DDT/LDPE blends, the maximum decomposition is less than 3.5 wt % before the beginning of the second decomposition process. It is obvious that through the blending process, the thermal stability could be greatly improved except the 20/80 blend.

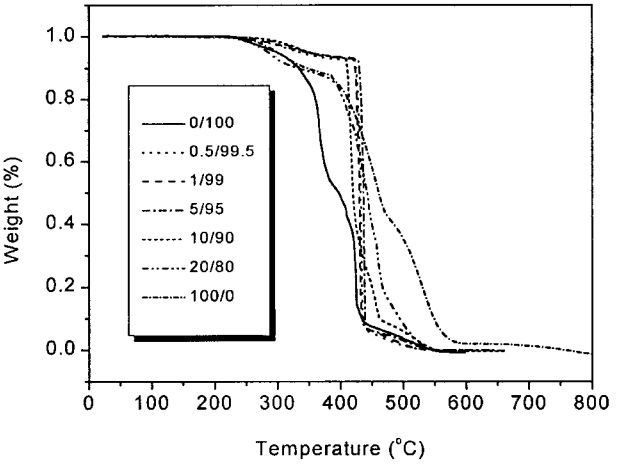

Figure 3 The results of thermogravimetric analysis of the neutral P3DDT/LDPE blends.

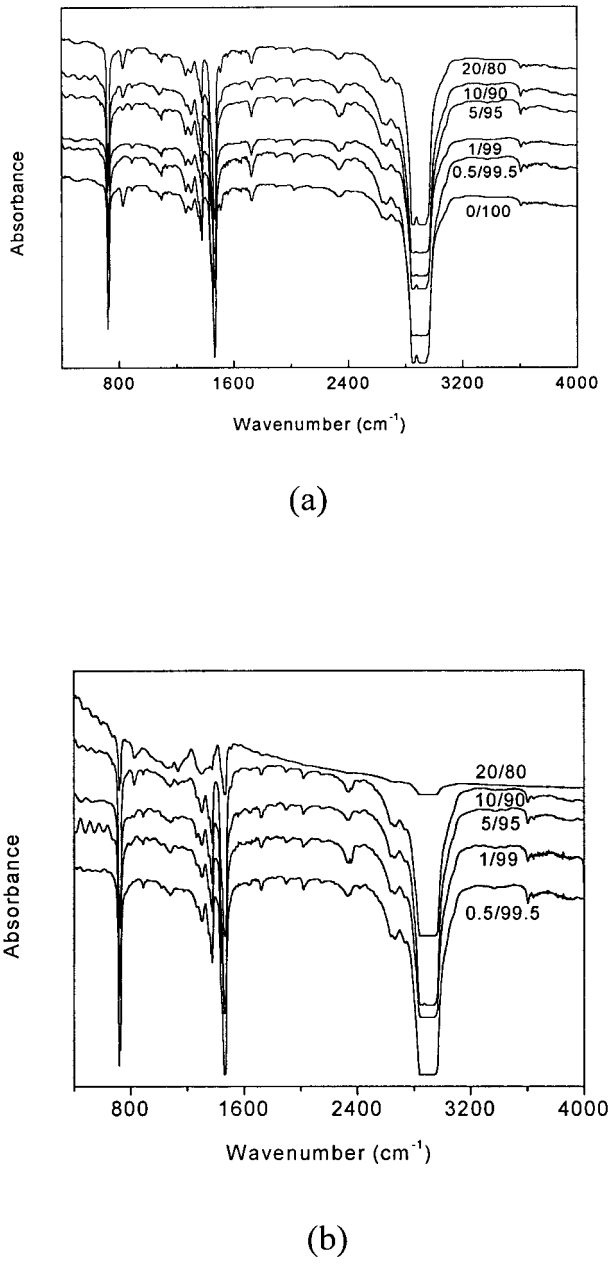

Figure 4 FTIR spectra of the neutral and doped P3DDT/LDPE blends: (a) the neutral blends; (b) the doped blends.

Fourier Transform Infrared Spectra

Figure 4 shows the FTIR spectra of the neutral and doped LDPE/P3DDT blends with different compositions. In common, the results of FTIR experiments can help to obtain important information on the detailed structure of polymers. In (a) of Figure 4, it can be observed that the FTIR spectra of these samples are very similar to one another, except that the absorption bands at 825 and 1508 cm^{-1} become obvious when the P3DDT composition is no less than 5%. The bands at 825 and 1508 cm^{-1}, which are the characteristic absorption bands of P3ATs,[18] correspond to the ═CH out-of-plane deformation of thiophene and the thiophene ring stretching mode, respectively. It could be also observed that with the increase of the composition of P3DDT, the intensities of its characteristic FTIR absorption bands become greater correspondingly. Thus it can be seen that P3DDT and LDPE represent their separate FTIR properties, and there is no obvious interaction between the molecular chains of P3DDT and LDPE.

In (b) of Figure 4, it can be noted that great changes take place merely for the 20/80 blend. After doping, for the bands characteristic of the vibrations of alkyl chain group, the peaks at 2922 and 2852 cm^{-1} decrease greatly in intensity, and the peak at 1376 cm^{-1} almost disappears. Meanwhile, the absorption bands in the regions of 1200–1300 and 900–1200 cm^{-1}, which belong to the CH_2 wagging mode and the C—C stretch mode, respectively, increase in intensity. During doping oxidation, the intervention of the dopant ion requires that both the alkyl side chains and the thiophene main chains undergo cooperative rotations to form a guest–host complex, and the resultant reorganization of polymer chains leads to infrared spectroscopy changes. It is worth mentioning that great increase in the intensities of the absorption bands at 1200–1300 and 900–1200 cm^{-1} should be attributed to the orientations of the side chain group. In addition, the change of the bands at 825 cm^{-1} should be attributed to the coupling of the skeletal backbone vibrations with the π-electron charge oscillations along the chains. During the doping oxidation, the dopant ion should have influence merely on P3DDT. However, for the blends containing smaller amount of P3DDT (less than 20%), changes in infrared spectroscopy have not appeared evident.

Scanning Electron Microscopy

Cryofractured surfaces of the neutral P3DDT/LDPE blends are shown in Figure 5. The morphology of these blends shows a uniform dispersion, and the degree of uniform dispersion increases with the increase of P3DDT content. When the P3DDT composition is increased, the strip morphology of P3DDT become obvious, and

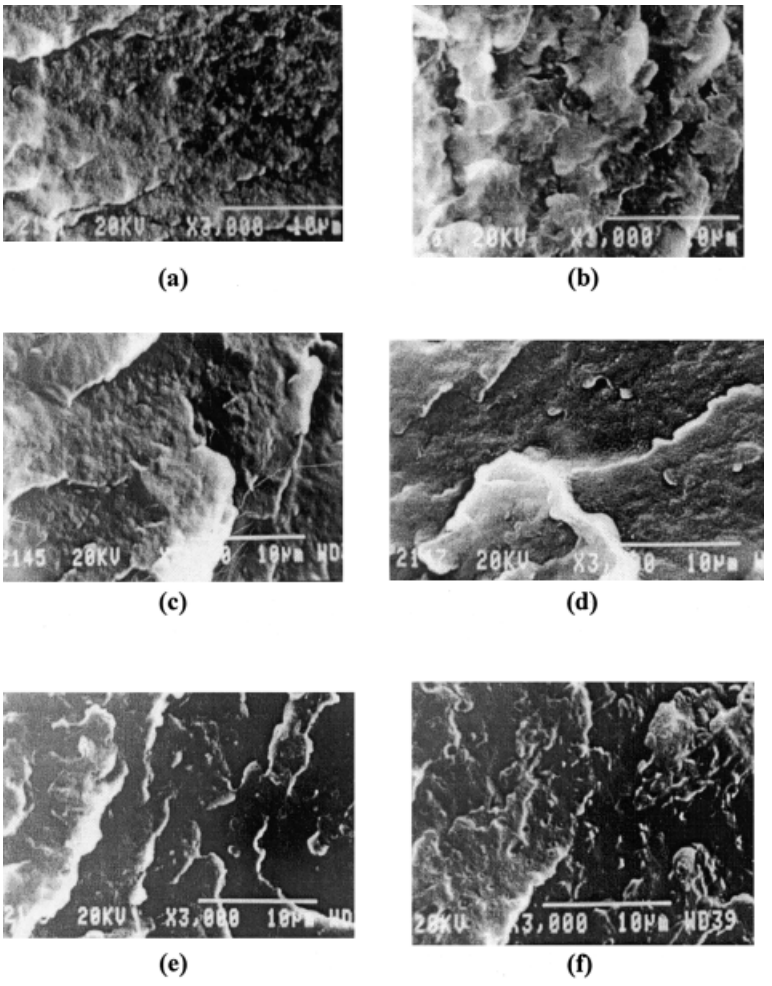

Figure 5 The SEM morphology of the neutral P3DDT/LDPE blends: (a) 0/100; (b) 0.5/99.5; (c) 1/99; (d) 5/95; (e) 10/90; (f) 20/80.

partially continuous phase of P3DDT begins to appear in the continuous phase of LDPE, which would indicate that the conductive paths of P3DDT have formed in the partial region of LDPE phase. In Figure 6, the SEM morphology of the doped P3DDT/LDPE blends is also shown. As indicated in Figure 6, after doping, a more uniform dispersion can be obtained, and the conductive paths are more obvious. Thus it can be seen that higher conductivity of the P3DDT/LDPE blends can be achieved after doping process.

Conductivity Measurements

As for the postdoped polymer blends, the conductivity would be controlled by the choice of the matrix polymer, the doping technique, the doping time, and the P3ATs content in the blends. For the blends in this paper, it is found that when the P3DDT content is no more than 5% in the blend, the conductivity has no favorite increase after a long-time solution doping. Although these blends have been immersed in nitromethane solution of anhydrous ferric chloride for a week, the conductivities of the doped blends are still very low. As is measured, the conductivities are 1.90×10^{-15} s/cm for the 0.5/99.5 blend, 2.31×10^{-15} s/cm for the 1/99 blend, and 2.62×10^{-11} s/cm for the 5/95 blend. While for the 10/90 and 20/80 blends, after doping for 3 days, values of conductivity can be up to 5.82×10^{-3} s/cm and 0.19 s/cm, respectively, as indicated in Figure 7. In Figure 7, values of conductivity of the pure P3DDT film with different doping time are also represented. The conductivity of doped P3DDT film amounts to 36.60 s/cm after 3 days doping. It can be found that within the same doping time, the conductivity of the

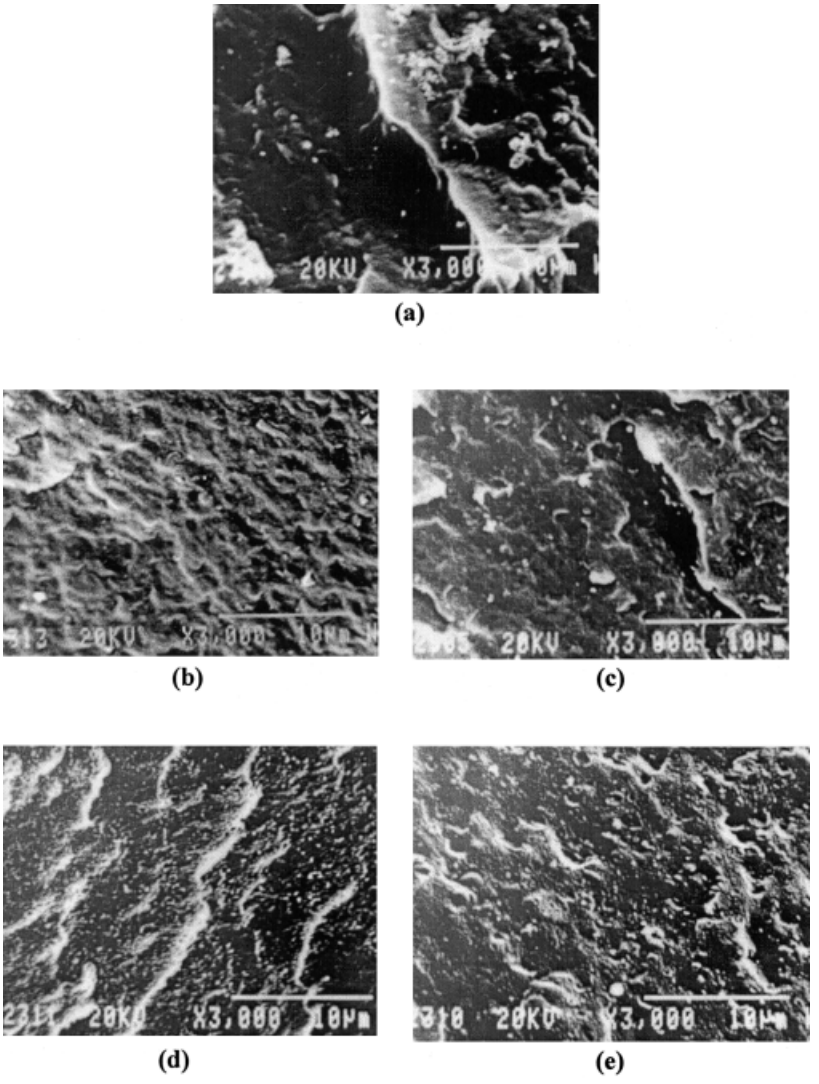

Figure 6 The SEM morphology of the doped P3DDT/LDPE blends: (a) 0.5/99.5; (b) 1/99; (c) 5/95; (d) 10/90; (e) 20/80.

blends increases with the increase of P3DDT composition, and for each sample the conductivity increases with the increase of doping time. It can also be observed that the curves in Figure 7 are steep before 10 h doping time and then become gentle later. From this it can be inferred that the doping process would tend to saturation when the samples have been doped for a certain period of time. For further study on the stability of these doped samples, the changes of the conductivity with the time at room temperature were also investigated for the doped 20/80 blend and pure P3DDT with different doping time, just as illustrated in Figure 8. Similar to the curves in Figure 7, the curves in Figure 8 are steep before 5 days first and then become gentle finally. Thus it can

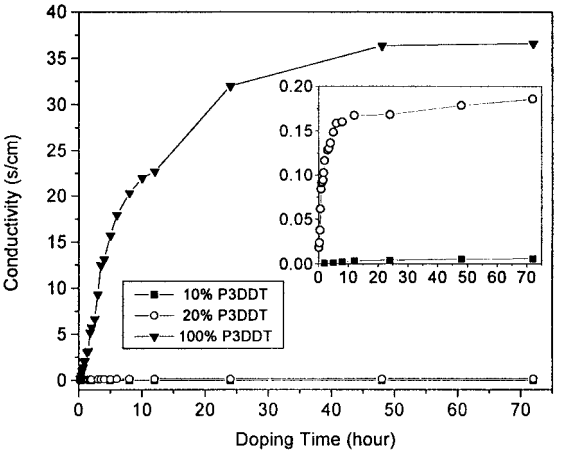

Figure 7 Conductivity of the doped P3DDT/LDPE blends with different doping time.

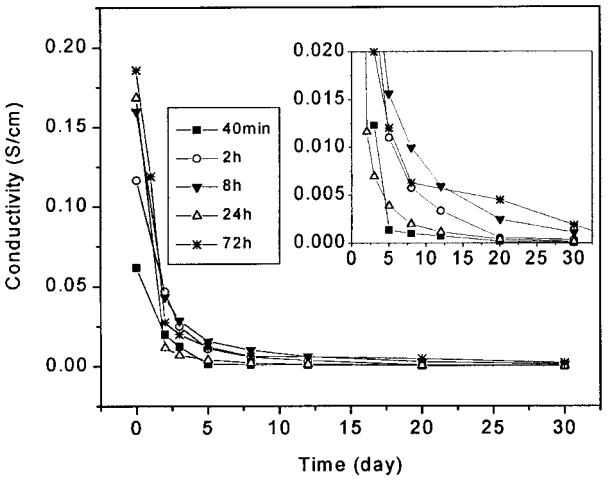

(a)

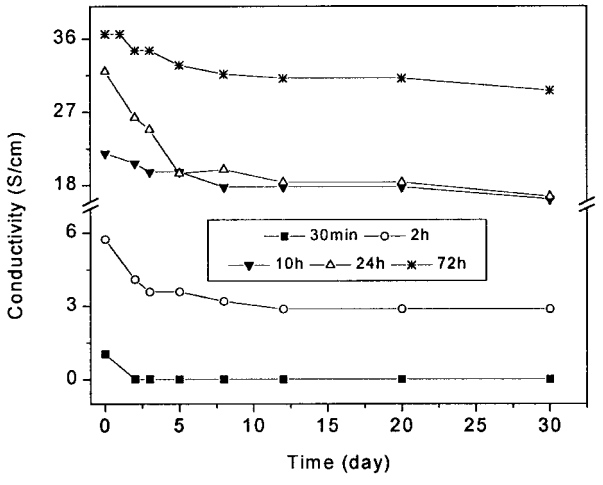

(b)

Figure 8 The conductivity stability of the doped samples with the time: 20/80 blend; (b) pure P3DDT.

be seen that the conductivity of these doped samples will turn to stabilization with the lengthening of time.

CONCLUSION

It has been demonstrated that separate crystallization occurs between P3DDT and LDPE during crystallization process, and it seems that there is almost no interaction between the molecular chains of P3DDT and LDPE. During the investigation of the thermal stability, it is found that the thermal stability of the blend becomes much better than that of the pure component, especially that of the 5/95 blend. In addition, there is some difference among the X-ray diffraction results of the blends, due to the nucleation reagent effect of small amount of P3DDT. It should be noted that P3DDT and LDPE show a uniform dispersion in SEM morphology. After doping, due to the increase of interaction force of molecular chains of P3DDT, more compact packing of molecular chains and more uniform dispersion in morphology can be obtained.

During the measurements of the conductivity, despite a long-time solution doping, only when the P3DDT content is more than 5% in the blend can the conductivity achieve a favorite increase. The conductivity increases with the increase of P3DDT content and the doping time. The study of the conductivity stability indicates that the conductivity decreases with the time, but will tend to stabilization gradually.

This investigation is subsidized by the Special Funds for Major State Basic Research Projects and the Chinese “863-2” high technology funds.

REFERENCES

1. Chiang, C. K.; Park, Y. W.; Heeger, A. J.; Shirakawa, H.; Louis, E. J.; MacDiarmid, A. G. Phys Rev Lett 1977, 39, 1098.
2. Diaz, A. F.; Kanazawa, K. K.; Gardini, G. P. J Chem Soc Chem Commun 1979, 14, 635.
3. Diaz, A. F.; Logan, J. A. Electroanal Chem 1980, 111, 111.
4. MacDiarmid, A. G.; Chiang, J. C.; Halpern, M.; Huang, H. S.; Su, S. L.; Somasiri, N. L. D.; Wu, W.; Yaniger, S. I. Mol Cryst Liq Cryst 1985, 121, 173.
5. Krische, B.; Zagorska, M. Synth Met 1989, 28, C263.
6. Sugimoto, R.; Takeda, S.; Gu, H. B.; Yoshino, K. Chem Express 1986, 1, 635.
7. Mo, Z. S.; Lee, K.-B.; Moon, Y. B.; Kobayashi, M.; Heeger, A. J.; Wudl, F. Macromolecules 1985, 18, 1972.
8. Elsenbaumer, R. L.; Jen, K. Y.; Oboodi, R. Synth Met 1986, 15, 169.

9. Kaeriyama, K.; Sato, M.; Tanaka, S. Synth Met 1987, 18, 233.
10. Chen, S.-A.; Ni, J.-M. Macromolecules 1992, 25, 6081.
11. Hsu, W.-P.; Levon, K.; Ho, K.-S.; Myerson, A. S.; Kwei, T. K. Macromolecules 1993, 26, 1318.
12. Laakso, J.; Osterholm, J.-E.; Nyholm, P.; Stubb, H.; Punkka, E. Synth Met 1990, 37, 145.
13. Laakso, J.; Osterholm, J. -E.; Nyholm, P. Synth Met 1989, 28, C467.
14. Ljungqvist, N.; Hjertberg, T. Synth Met 1993, 55–57, 4944.
15. Tamao, K.; Kodama, S.; Nakajima, I.; Kumada, M. Tetrahedron 1982, 38, 3347.
16. Osterholm, J. E.; Passiniemi, P.; Isotalo, H.; Stubb, H. Synth Met 1987, 18, 213.
17. Kawai, T.; Nakazono, M.; Sugimoto, R.; Yoshino, K. Synth Met 1993, 55–57, 353.
18. Winokur, M. J.; Spiegel, D.; Kim, Y.; Hotta, S.; Heeger, A. J. Synth Met 1989, 28, C419.